Carotid blood flow measurement accelerated by compressed sensing

Magnetic Resonance Imaging 31 (2013) 1485–1491

Contents lists available at ScienceDirect

Magnetic Resonance Imaging

journal homepage: www.mrijournal.com

Carotid blood flow measurement accelerated by compressed sensing: Validation in healthy volunteers ☆

Yuehui Tao [a], Gabriel Rilling [b], Mike Davies [b], Ian Marshall [c,d,*]

[a] Oxford Centre for Clinical Magnetic Resonance Research, University of Oxford, Oxford, UK
[b] Institute of Digital Communications, School of Engineering and Electronics, University of Edinburgh, Edinburgh, UK
[c] Centre for Clinical Brain Sciences, University of Edinburgh, Edinburgh, UK
[d] University and British Heart Foundation Centre for Cardiovascular Science, University of Edinburgh, Edinburgh, UK

ARTICLE INFO

Article history:
Received 3 May 2013
Revised 28 May 2013
Accepted 28 May 2013

Keywords:
Carotid arteries
Carotid flow
Compressed sensing
Phase contrast
Acceleration
Cine phase contrast

ABSTRACT

Measurement of blood flow by cine phase-contrast MRI is a valuable technique in the study of arterial disease but is time consuming, especially for multi-slice (4D) studies. Compressed sensing is a modern signal processing technique that exploits sparse signal representations to enable sampling at lower than the conventional Nyquist rate. It is emerging as a powerful technique for the acceleration of MRI acquisition. In this study we evaluated the accuracy of phase-contrast carotid blood flow measurement in healthy volunteers using threefold undersampling of kt-space and compressed sensing reconstruction.

Sixteen healthy volunteers were scanned at 1.5 T with a retrospectively gated 2D cine phase-contrast sequence. Both fully sampled and three-fold accelerated scans were carried out to measure blood flow velocities in the common carotid arteries. The accelerated scans used a k-t variable density randomised sampling scheme and standard compressed sensing reconstruction. Flow rates were determined by integration of velocities within the manually segmented arteries. Undersampled measurements were compared with fully sampled results.

Bland–Altman analysis found that peak velocities and flow rates determined from the compressed sensing scans were underestimated by 5% compared with fully sampled scanning. The corresponding figure for time-averaged flow was 3%.

These acceptably small errors with a threefold reduction in scan time will facilitate future extension to 4D flow studies in clinical research and practice.

1. Background

Carotid arterial blood velocity mapping can be used for the diagnosis and management of the progression of carotid artery atherosclerosis, which is one of the major causes of ischaemic stroke [1]. Time-resolved flow rates in carotid arteries provide useful information on cerebral circulation and are also used as boundary conditions for computational fluid dynamics models [2,3]. Flow measurements in other major arteries are also of clinical interest. As with other dynamic imaging techniques, the 2D cine phase-contrast MRI sequence used for flow measurement is slow due to the coverage of the extra temporal and velocity encoding dimensions of the signal, requiring a trade-off between spatial and temporal resolution. Extending the technique to multiple slices leads to long scan times (tens of minutes) that introduce measurement errors from patient motion and physiological variation, and are infeasible in a clinical setting. The availability of robust, accelerated scanning is therefore necessary before these techniques can be used clinically. Methods to accelerate MRI acquisition include parallel imaging [4,5], lattice-based kt-undersampling such as UNFOLD [6] and kt-BLAST [7], and compressed sensing (CS) [8–11]. Compressed sensing is a framework of undersampling and reconstruction methods for recovering sparse signals sampled at a rate lower than the Nyquist rate. Most MRI datasets are sparse in the Fourier (k-space) domain, with most of the signal power lying near the centre of k-space. Angiograms are sparse in the image domain itself, with relatively few pixels contributing to the image. Recent studies have reported promising results for various compressed sensing applications, including contrast enhanced angiography [11], cardiac imaging [12], cardiac output measurement [13], and blood flow measurement in hepatic veins [14] and the aorta [15]. Preliminary implementation of the CS framework in carotid velocity mapping has also demonstrated good undersampling performance [16], but to date the technique has not been properly

* Corresponding author.
E-mail addresses: yuehui.tao@cardiov.ox.ac.uk (Y. Tao), g.rilling@ed.ac.uk (G. Rilling), mike.davies@ed.ac.uk (M. Davies), ian.marshall@ed.ac.uk (I. Marshall).

0730-725X/$ – see front matter © 2013 The Authors. Published by Elsevier Inc. All rights reserved.
http://dx.doi.org/10.1016/j.mri.2013.05.009

validated in these vessels. Clinically, it is highly desirable to understand the accuracy and reliability of such a strategy before it could be used to guide treatment. However, current CS theory does not provide quantitative guidance as to how much error should be expected for specific MR applications. In this study, we applied the CS method to accelerate carotid velocity and flow rate measurements in healthy volunteers. The CS results for peak and time-averaged flow were compared with measurements from corresponding fully sampled scans. To the best of our knowledge this is the first in vivo validation of CS for carotid flow measurement.

2. Methods

2.1. Design of undersampling pattern

Central to undersampling techniques is the design of a suitable k(-t) undersampling pattern. Although there is no comprehensive theory for the design of k-t sampling patterns, it is well known that full sampling near the centre is advantageous [17,18] because the majority of the signal power lies in the central region. Furthermore, compressed sensing undersampling factors in the range 2–5 appear to give acceptable results for phase-contrast applications [13–16], and for compressed sensing reconstruction the sampling pattern should be incoherent [8–11]. Therefore, we designed a sampling pattern similar to those used previously [15,16], having an overall acceleration factor of three with full sampling of the central 20 rows of k-t space and the remaining k-t space being sampled with a uniform density, randomised pattern. This pattern is shown in Fig. 1 together with the fully sampled pattern. Preliminary simulations (data not shown) based on undersampling the fully sampled signal from one volunteer confirmed that the pattern was suitable, with a performance comparable to the more complex patterns used by Kim et al [14]. Furthermore, different randomisations with the same sampling density gave near-identical results.

2.2. Cine phase-contrast scanning

Sixteen healthy volunteers (nine female and seven male, age 38 ± 9) were recruited for the study. Informed consent was obtained from all volunteers and the protocol for the scans was approved by a Local Research Ethics Committee. All imaging used a 1.5T GE Signa Horizon HDX scanner operating under a research collaboration with GE Medical Systems (Milwaukee, WI, USA) and fitted with a four-element phased array carotid surface coil (Machnet, Netherlands). The manufacturer's standard 2D cine phase-contrast pulse sequence program (with alternating velocity-compensated and velocity-encoded acquisitions) was modified to incorporate the compressed sensing pattern. After localiser scans and a Time of Flight angiographic scan to visualise the carotid arteries, 24 time frames of a single axial slice (matrix 192×192) located approximately 2 mm below the lower of the two carotid bifurcations were collected in each phase-contrast acquisition. Retrospective gating used a pulse oximeter attached to the right index finger of the volunteer. Velocity encoding was applied only in the Superior/Inferior direction (S/I), with phase encoding in the Anterior/Posterior direction (A/P, defined as y) and frequency encoding in the Left/Right direction (L/R, defined as x). Other parameters were field of view 12 cm, slice thickness 2 mm, VENC 100 cm/s, acquisition bandwidth 15.63 kHz, repetition time 16 ms, echo time 7.8 ms and flip angle 25º. Each volunteer had three scans in the same visit, consisting of two fully sampled scans separated by the CS scan. The three scans were run back-to-back without changing the scanner's shim or gain settings. Each fully sampled scan took 147 seconds, and the CS scan took 49 seconds. Trigger pulses from the oximeter and the scanner were logged by an event recorder (Cambridge Electronic Design, Cambridge, UK). Raw k-space data was saved for offline reconstruction.

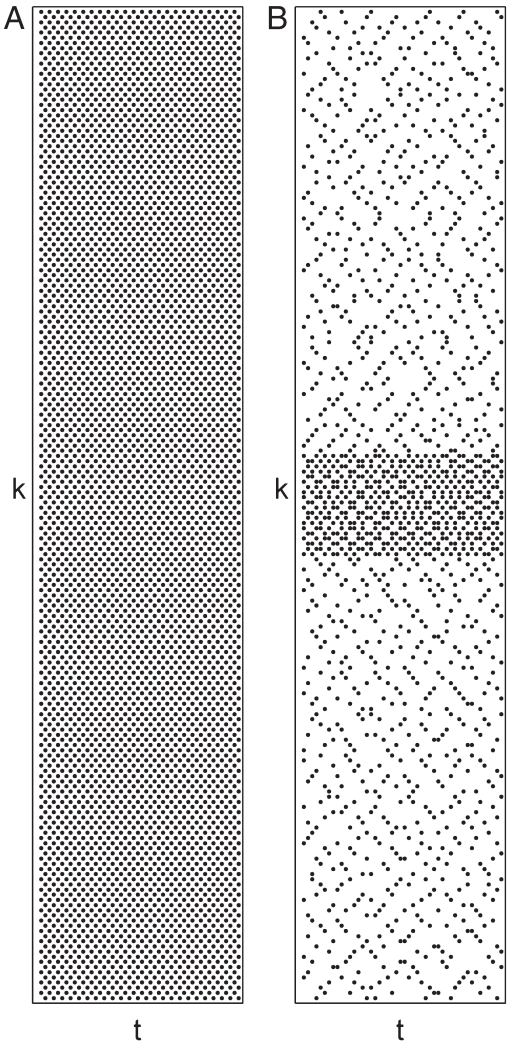

Fig. 1. Sampling patterns. (A) Fully sampled and (B) Compressed Sensing (CS) sampling patterns in kt-space. Each dot represents a frequency encoding line. The CS pattern has 20 central rows densely sampled, whilst the remainder of kt-space is sampled randomly with a uniform density such that the overall acceleration factor is three.

2.3. Image reconstruction and analysis

Data was reconstructed offline according to the pulse sequence timing and the gating record from the pulse oximeter. For each volunteer and each common carotid artery, the signal from the closest coil element was used. Velocity-compensated and velocity-encoded signals were reconstructed separately. For reconstruction of the fully sampled scans, regridding of the data to 24 time frames by cubic interpolation was carried out at each phase encoding position, followed by 2-dimensional Fourier transformation into image space. For reconstruction of the CS scans, the L1 norm was minimized in y-f space (Fourier transform of k-t space) using the SPGL1 package [19]. Each of 18 locations in the x-direction, spanning the region occupied by a carotid artery, was processed separately, and the process was repeated for right and left arteries. In each reconstruction, regridding of the undersampled signal provided an initial estimate for the SPGL1 algorithm. The computation used Matlab (MathWorks, Natick, MA, USA) running on a PC (3.2GHz Intel Xeon CPU with 2 GB RAM). The reconstruction for

each CS scan took approximately 5 minutes. All carotid arteries were segmented manually by the same observer to ensure consistency. This was done independently for each scan of each volunteer. Pixel-by-pixel velocities were calculated for all pixels included in the vessel segmentations, and any phase wraps around the time of peak flow were automatically corrected. Vessel flow rates were determined by summing the velocities within the arteries and multiplying by the pixel area. For each volunteer and each artery the peak velocities, peak flow rates and time-averaged flow rates from the two fully sampled scans were averaged and used as a reference for comparison with the results from the undersampled CS scan in between. Since the differences between the CS results and the reference include real physiological variations between scans in addition to any errors due to undersampling, the differences between the two fully sampled measurements were also evaluated. Bland-Altman analysis was also carried out on the flow rates.

3. Results

One volunteer moved excessively during scanning and the images were judged to be of poor quality. The remaining 15 volunteers were included in the subsequent analysis. A representative neck image, together with zoomed views of the common carotid arteries and pixel-wise velocity waveforms, are shown in Fig. 2. Velocity waveforms for the fully sampled and compressed sensing scans are shown for the central 5×5 pixels of the RCCA in Fig. 3(a), and the corresponding flow waveform in Fig. 3(b). This volunteer had a high flow rate (9.8 ml/s time-averaged) compared with the more "typical" value of 6.0 ml/s shown in Fig. 3(c) and the low value of 4.5 ml/s shown in Fig. 3(d).

Velocity and flow results are summarised in Table 1 and illustrated in Figs. 4 and 5. Peak velocities were slightly underestimated by the CS scan but the difference reached significance ($p < 0.05$) only for the LCCA (3.8 cm/s or 5% underestimation). Fig. 4(a,b) show the differences in flow waveforms between the CS results and the average of those from the two fully sampled scans. Around peak flow, the differences (averaged over all volunteers) were approximately -1 ml/s but with large standard deviations (2 ml/s) reflecting the fact that peak flow did not occur at the same time point for all volunteers. During diastole, the differences were less than (0.03 ± 0.4) ml/s. Flow differences between the results from the two fully sampled scans are also presented in Fig. 4(c,d) to indicate the level of scan to scan variation. Between the two fully sampled scans, the mean differences were less than 0.5 ml/s at peak flow and 0.1 ml/s during diastole. Again, the standard deviations at peak

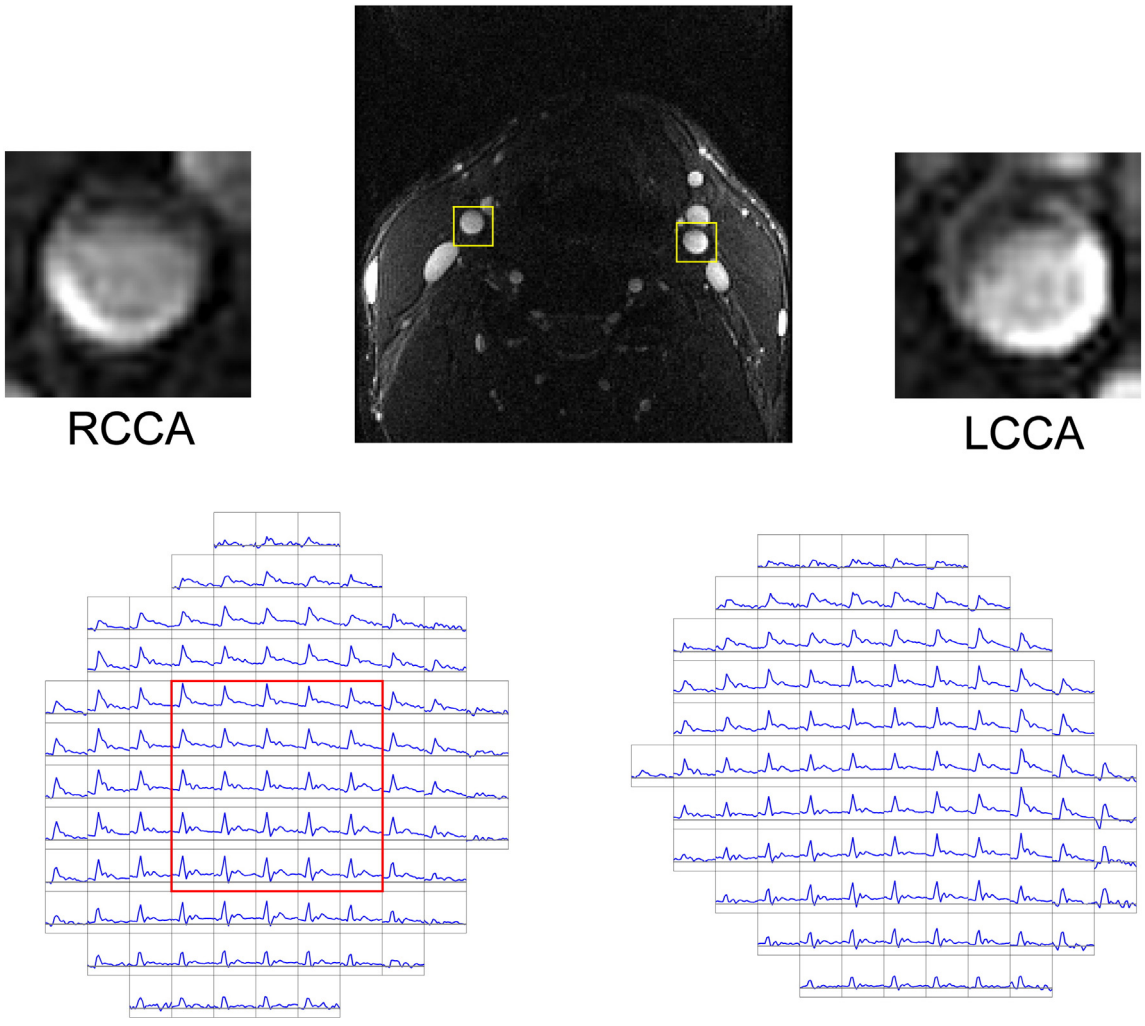

Fig. 2. Common carotid artery images and pixel-wise velocity waveforms. Representative results from a subject with high carotid artery flow. The upper panel shows magnitude images of the entire neck together with zoomed views of the common carotid artery (CCA) regions of interest (outlined in yellow in the neck image). The CCA images have been interpolated for the display purposes. The lower panel shows pixel-wise velocity waveforms in the arteries, corresponding to the first fully sampled scan. Waveforms are shown only for those pixels within the segmented arteries. The velocity scale is from −30 cm/s to 110 cm/s. The red outline depicts the central pixels displayed in detail in Fig. 3(A).

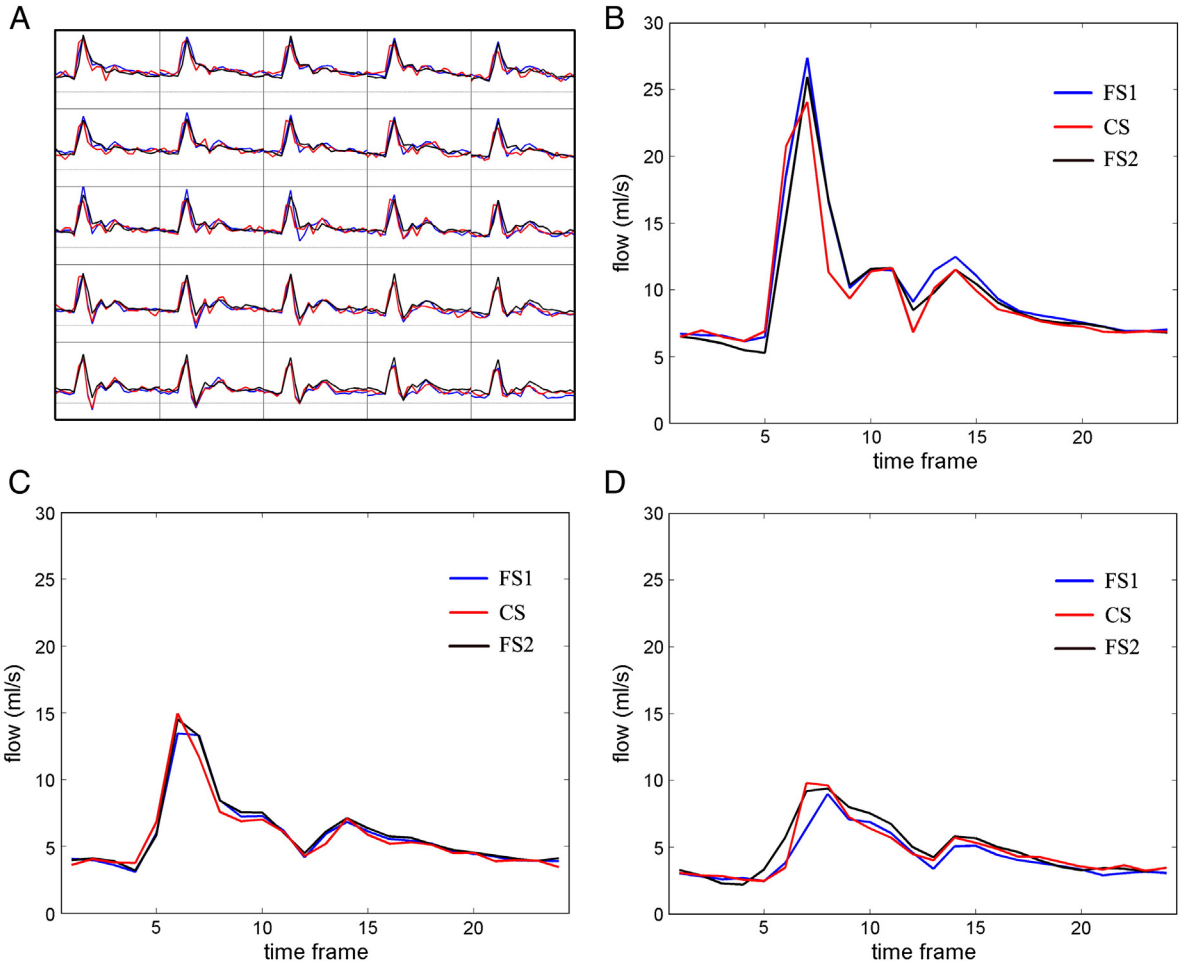

Fig. 3. Velocity and flow waveforms in representative subjects. (A) Pixel-wise velocity waveforms for the central region of the right CCA as depicted by the red outline in Fig. 2, in a subject with relatively high carotid flow rates. In all panels of this figure, the first fully sampled scan FS1 is shown with a blue line, the threefold undersampled compressed sensing scan CS is shown with a red line and the second fully sampled scan FS2 is shown with a black line. The velocity scale is from −30 cm/s to 110 cm/s. (B) RCCA flow waveforms for the same subject; (C) RCCA flow waveforms for a subject with moderate flow rates; (D) RCCA flow waveforms for a subject with low flow rates. Flow was determined by summing the individual pixel velocities within the arteries and multiplying by the pixel area.

flow are approximately 2 ml/s. Fig. 5 shows Bland-Altman plots comparing the CS and fully-sampled results for (a) peak flow and (b) time-averaged flow. In this figure, data for right and left CCA are plotted on the same axes, but they are reported separately in Table 1. There was a significant bias (underestimation) in peak flow measured using the CS scan compared with the mean fully sampled scans of (0.77 ± 1.03) ml/s for RCCA and (0.73 ± 1.14) ml/s for LCCA. Time-averaged flow rates measured by the CS scans were underestimated by approximately 0.18 ml/s compared with the mean fully sampled scans, but the difference reached significance only for the RCCA. Linear regression analysis of the Bland-Altman plots revealed weak but significant ($p < 0.01$) negative correlations between flow rate differences (CS-mean fully sampled) and the mean fully sampled flow rates ($R^2 = 0.31$ for peak flow and 0.23 for time-averaged flow).

4. Discussion

Common carotid artery flow waveforms were successfully measured using threefold accelerated CS. Waveform shapes

Table 1
Summary flow results.

		FS1	FS2	FS1-FS2	CS	CS- < FS>
Peak velocity (cm/s)	RCCA	74.4 ± 19.5	76.2 ± 17.0	-1.7 ± 5.8	73.5 ± 14.2	-1.8 ± 8.2
Peak velocity (cm/s)	LCCA	74.4 ± 16.5	75.8 ± 19.9	-1.5 ± 12.1	71.3 ± 15.3	**-3.8 ± 5.8**
Peak Flow (ml/s)	RCCA	14.2 ± 5.2	14.5 ± 4.8	-0.23 ± 1.27	13.6 ± 4.3	**-0.77 ± 1.03**
Peak Flow (ml/s)	LCCA	14.5 ± 4.9	15.0 ± 4.9	-0.57 ± 1.11	14.0 ± 4.4	**-0.73 ± 1.14**
Time-averaged flow (ml/s)	RCCA	6.21 ± 1.48	6.39 ± 1.46	-0.18 ± 0.36	6.10 ± 1.32	**-0.19 ± 0.23**
Time-averaged flow (ml/s)	LCCA	6.47 ± 1.47	6.59 ± 1.55	-0.12 ± 0.36	6.36 ± 1.41	-0.17 ± 0.34

Common Carotid Artery (CCA) peak velocities (cm/s), peak and time-averaged flow rates (ml/s) measured with fully sampled and threefold accelerated cine-PC scans. All values are mean (± standard deviation) for n = 15 subjects. FS1, first fully sampled scan; FS2, second fully sampled scan; CS, threefold undersampled scan with compressed sensing reconstruction; <FS>, mean of FS1 and FS2. Values in **bold** are significantly different from zero ($p < 0.05$). See also Figs. 4 and 5.

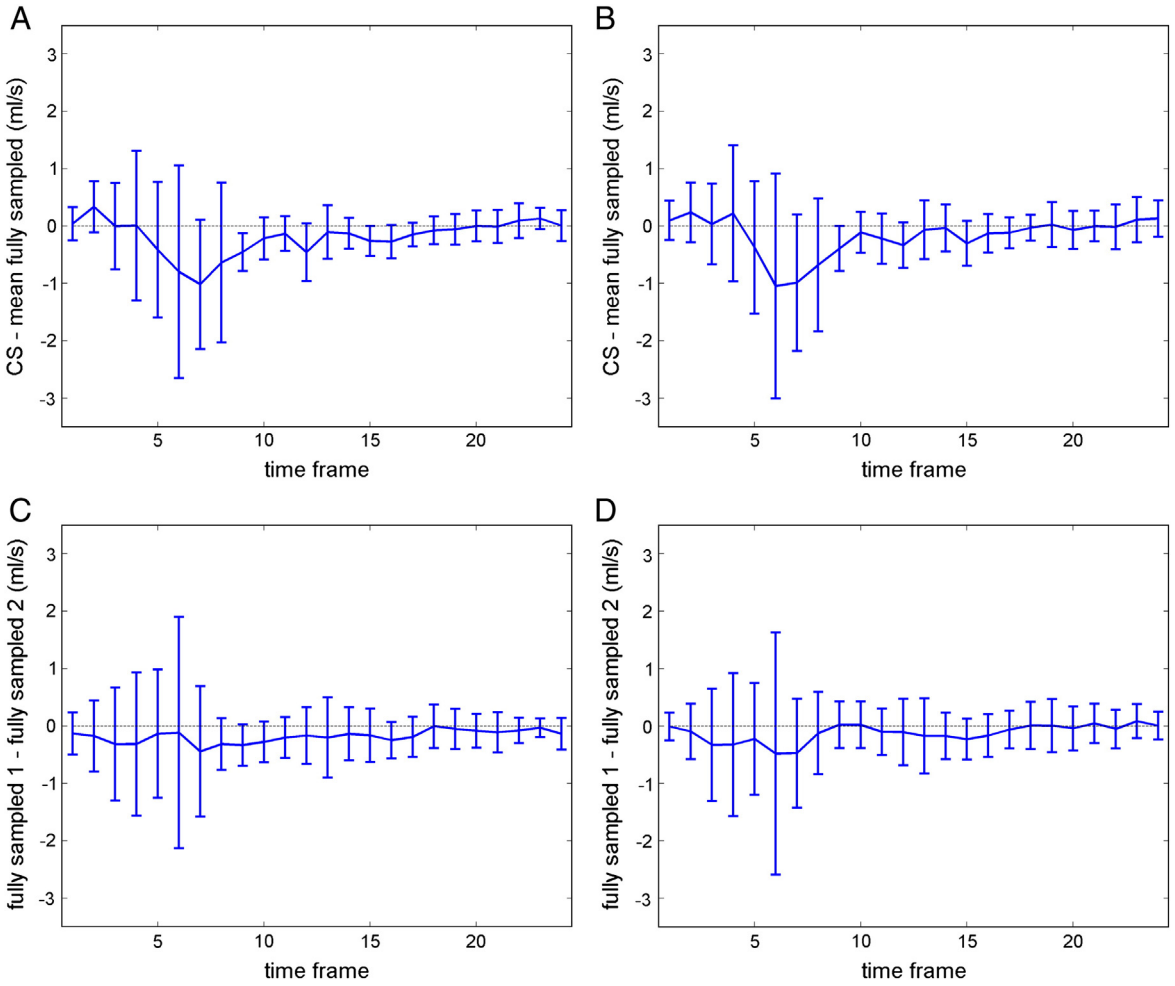

Fig. 4. Compressed sensing versus fully sampled flow waveforms. The differences in measured common carotid artery (CCA) flow waveforms between (A, B) the threefold-accelerated CS results and the average of those from the two fully sampled scans, and (C, D) between the two fully sampled scans. Results for the right CCA are shown in (A) and (C), and results for the left CCA in (B) and (D). Each error bar shows one standard deviation above and below the mean difference, calculated over all 15 volunteers. See also Table 1.

(Fig. 3) and flow rates were similar to previous work [20,21] and the waveforms from the CS scans showed good agreement with the waveforms from the fully sampled scans.

The group mean underestimation of approximately 1 ml/s at peak flow for the CS scans had a spread of ± 2 ml/s that arises partly because the time of peak flow did not occur at the same time point for all volunteers and all scans, as can be observed in Fig. 3. When the individual peak flow rates are used (regardless of exact timing in the waveforms), as in the Bland-Altman analysis, the underestimation is 0.75 ml/s with a standard deviation of just over 1 ml/s, i.e. less variation than for group means. Although significant ($p < 0.05$), this underestimation amounts to only 5% of the typical peak flow rate of 14.5 ± 5 ml/s. This underestimation probably arises because smaller coefficients (relating to higher frequency signal components) tend to be underestimated during the compressed sensing reconstruction. This in turn leads to reduced temporal resolution resulting in a broader but smaller peak in the flow waveform. Since velocities are extracted from the phase of the voxels, it can be shown that the same mechanism may also lead to underestimation of the time average of waveforms having a distinct pulsatile peak such as those studied here. This probably explains the underestimation of 0.18 ml/s (3%) observed in the time-averaged flow rates.

When selecting patients for carotid surgery, important thresholds for (internal) carotid artery disease are 50% and 70% (diameter) stenosis, for which the observed peak velocities will be approximately four and eleven times healthy values respectively. In this context, a 5% underestimation of velocities will have negligible effect on diagnosis, and it may be that higher acceleration factors are achievable.

We used a relatively thin imaging slice of 2 mm thickness. The high inflow intensity in the common carotid arteries led to adequate signal to noise and velocity to noise ratios. This may not be the case in regions of lower flow velocity, such as downstream of the carotid bifurcation, for which more sophisticated compressed sensing techniques may be necessary to ensure adequate phase reconstruction [22]. The time saving of approximately 100 seconds for the single slice in this study may seem rather modest in the context of an MRI examination. However, our interest is in exploring the flow patterns in extended arterial regions for which a multi-slice or 3-dimensional approach will be appropriate. Extending the examination to measure all three components of velocity in a stack of slices ("4D acquisition") leads to clinically unfeasible examination times unless some form of acceleration is employed. With the threefold acceleration demonstrated here, each slice takes approximately 50 s to acquire, so that a stack of, say, 12 slices covering the carotid bifurcation region could be achieved in a comfortable ten minute scan. It is expected that the compressed sensing reconstruction would benefit from the 3D structure in such data.

In the current implementation, the general form of the compressed sensing method was used to exploit the general sparsity

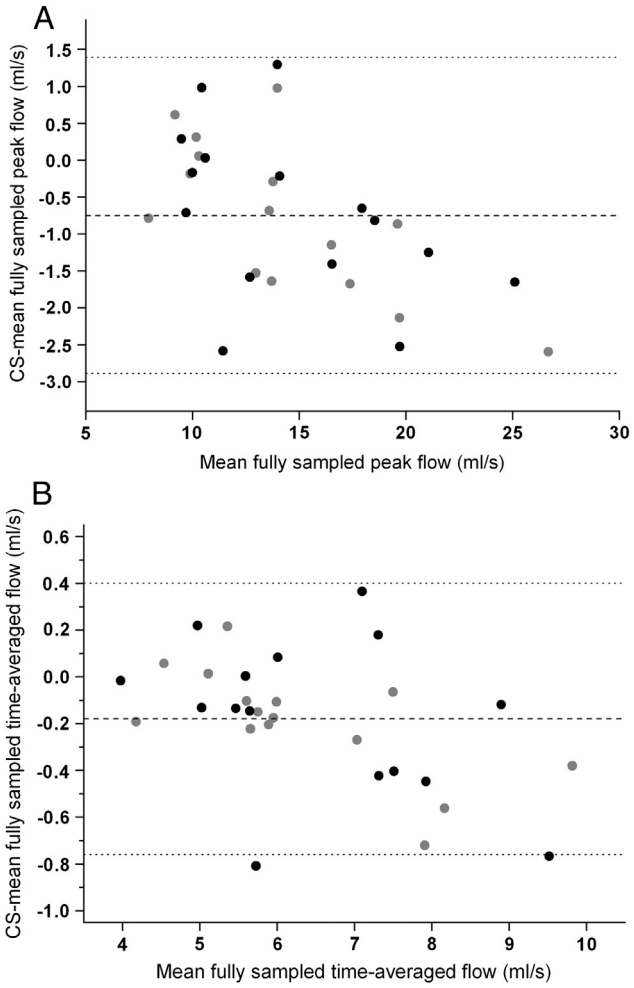

Fig. 5. Bland Altman diagrams of peak and time-averaged flow rates. The differences in measured common carotid artery (CCA) flow rates between the threefold-accelerated CS results and the average of those from the two fully sampled scans. Results for peak flow are shown in (a) and for time-averaged flow in (b). Mean biases are shown with dashed lines, whilst dotted lines represent ± two standard deviations. Data points for RCCA are shown in grey and for LCCA in black.

of the signal. No prior information or modelling of the signal was used in the reconstruction.

We used the Fourier Transform (FT) as the sparsifying transform. Although it has been reported that a Principal Components Analysis (PCA) transform may give better results [14], the reconstruction times would have been much greater. The relative merits of FT and PCA still need to be explored with a pool of fully sampled in vivo data such as the current study has generated. We did not use Total Variation (TV) regularisation in the reconstructions [22] because TV has a smoothing effect. This aspect was noted by Kwak et al [15] who were interested only in time-averaged volume flow. In our work we specifically wanted to retain spatially resolved velocity waveforms for further haemodynamic analysis.

Improvements in performance might be possible by using a joint reconstruction of the velocity-compensated and velocity-encoded signals [14] or by explicitly using the sparsity of the complex difference images [15]. Further acceleration would be possible by combining compressed sensing with parallel imaging [14], but we wanted to establish the baseline performance of CS alone. Furthermore, the phased array carotid coil used in this work behaved effectively as separate surface coils since signals from the left carotid artery were hardly detectable with the right-sided coil elements and vice versa. Future work would also explore different sampling density distributions and/or levels of acceleration, different sparsifying transforms, and a comparison with the kt-BLAST technique. The fully sampled data collected in the current study could be used for simulations of such undersampling Finally, in addition to healthy volunteers, patients with abnormal carotid blood flow should be included in future work prior to establishing routine clinical studies.

5. Conclusions

Threefold accelerated compressed sensing scans produced accurate measurements of time-resolved velocities and flow rates in common carotid arteries of healthy volunteers. Peak (time-averaged) flow rates were underestimated by 5 (3) % compared with fully sampled scanning, with a time saving of 100 seconds per slice. Such a reduction in scan time will facilitate the extension to multi-slice (4D) flow studies in clinical research and practice.

Acknowledgments

This work was funded by the Engineering and Physical Sciences Research Council (Grant EP/F039697/1) and the European Commission through the SMALL project under FET-Open (Grant 225913). Imaging (CRF reference E08641) was carried out at the Brain Research Imaging Centre, University of Edinburgh (www.bric.ed.ac.uk, which is part of the SINAPSE (Scottish Imaging Network - A Platform for Scientific Excellence) collaboration (www.sinapse.ac.uk) funded by the Scottish Funding Council and the Chief Scientist Office. Support from NHS Lothian R&D and the WTCRF are gratefully acknowledged. We also wish to thank the volunteers and the research radiographers.

References

[1] O'Rourke RA, Fuster V, Alexander RW, et al. Hurst's The heart manual of cardiology. . 11th Ed. New York: McGraw-Hill; 2005.
[2] Steinman DA, Thomas JB, Ladak HM, Milner JS, Rutt BK, Spence JD. Reconstruction of carotid bifurcation hemodynamics and wall thickness using computational fluid dynamics and MRI. Magn Reson Med 2002;47:149–59.
[3] Marshall I, Zhao S, Papathanasopoulou P, Hoskins P, Xu Y. MRI and CFD studies of pulsatile flow in healthy and stenosed carotid bifurcation models. J Biomech 2004;37:679–87.
[4] Sodickson DK, Manning WJ. Simultaneous acquisition of spatial harmonics (SMASH): fast imaging with radiofrequency coil arrays. Magn Reson Med 1997;38:591–603.
[5] Pruessmann KP, Weiger M, Scheidegger MB, Boesiger P. SENSE: Sensitivity encoding for fast MRI. Magn Reson Med 1999;42:952–62.
[6] Madore B, Glover GH, Pelc NJ. Unaliasing by Fourier-encoding the overlaps using the temporal dimension (UNFOLD), applied to cardiac imaging and fMRI. Magn Reson Med 1999;42:813–28.
[7] Kozerke S, Tsao J, Razavi R, Boesiger P. Accelerating cardiac Cine 3D Imaging using k-t BLAST. Magn Reson Med 2004;52:19–26.
[8] Candes E, Romberg J, Tao T. Robust uncertainty principles: Exact signal reconstruction from highly incomplete frequency information. IEEE Trans Info Theory 2006;52:489–509.
[9] Donoho DL. Compressed sensing. IEEE Trans Inform Theory 2006;52:1289–306.
[10] Candes E, Wakin MB. An introduction to compressive sampling. IEEE Signal Process Magn 2008;25:21–30.
[11] Lustig M, Donoho D, Pauly JM. Sparse MRI: the application of compressed sensing for rapid MR imaging. Magn Reson Med 2007;58:1182–95.
[12] Gamper U, Boesiger P, Kozerke S. Compressed sensing in dynamic MRI. Magn Reson Med 2008;59:365–73.
[13] Hsiao A, Lustig M, Alley MT, Murphy M, Vasanawala SS. Quantitative assessment of blood flow with 4D phase-contrast MRI and autocalibrating parallel imaging compressed sensing. In: Proceedings of ISMRM 19th Annual Meeting, Montreal, Canada, 2011:1190.
[14] Kim D, Dyvorne HA, Otazo R, Feng L, Sodickson DK, Lee VS. Accelerated phase-contrast cine MRI using k-t SPARSE-SENSE. Magn Reson Med 2012;67:1054–64.
[15] Kwak Y, Nam S, Akcakaya M, Basha TA, Goddu B, Manning WJ, Tarokh V, Nezafat R. Accelertaed aortic flow assessment with compressed sensing with and without use of the sparsity of the complex difference image. Magn Reson Med, DOI: http://dx.doi.org/10.1002/mrm.24514
[16] Tao Y, Rilling G, Daves M, Marshall I. Compressed sensing reconstruction with retrospectively gated sampling patterns for velocity measurement of carotid blood flow. In: Proceedings of ISMRM-ESMRMB Joint Annual Meeting, Stockholm, Sweden, 2010: 4866.

[17] Greiser A, von Kienlin M. Efficient k-space sampling by density-weighted phase-encoding. Magn Reson Med 2003;50:1266–75.
[18] Seeger M, Nickisch H, Pohmann R, Schölkopf B. Optimization of k-space trajectories for compressed sensing by Bayesian experimental design. Magn Reson Med 2010;63:116–26.
[19] van den Berg E, Friedlander PM. Probing the Pareto frontier for basis pursuit solutions. SIAM J Sci Comput 2008;31:890–912.
[20] Marshall I, Papathanasopoulou P, Wartolowska K. Carotid flow rates and flow division at the bifurcation in healthy volunteers. Physiol Meas 2004;25:691–7.
[21] Dean CR, Markus HS. Colour velocity flow measurement: in vitro validation and application to human carotid arteries. Ultrasound Med Biol 1997;23:447–52.
[22] Santelli C, Kozerke S, Schaeffter T. On compressed sensing for phase-contrast velocity mapping. In: Proceedings of ISMRM 20th Annual Meeting, Melbourne, Australia, 2012: 4204.